PHYSICAL REVIEW B **83**, 020502(R) (2011)

Charge transport through ultrasmall single and double Josephson junctions coupled to resonant modes of the electromagnetic environment

Yu. A. Pashkin,[1,2,*] H. Im,[2,3] J. Leppäkangas,[4] T. F. Li,[2,5] O. Astafiev,[1,2] A. A. Abdumalikov Jr.,[2] E. Thuneberg,[6] and J. S. Tsai[1,2]

[1]*NEC Green Innovation Research Laboratories, Tsukuba, Ibaraki 305-8501, Japan*

[2]*RIKEN Advanced Science Institute, Tsukuba, Ibaraki 305-8501, Japan*

[3]*Department of Semiconductor Science, Dongguk University, Phil-Dong, Seoul 100-715, Korea*

[4]*Institut für Theoretische Festkörperphysik and DFG Center for Functional Nanostructures (CFN), Karlsruhe Institute of Technology, D-76128 Karlsruhe, Germany*

[5]*Institute of Microelectronics, Tsinghua University, Beijing 100084, China*

[6]*Department of Physical Sciences, University of Oulu, FI-90014 Oulu, Finland*

(Received 6 October 2010; revised manuscript received 7 December 2010; published 20 January 2011)

We have investigated charge transport in ultrasmall superconducting single and double Josephson junctions coupled to resonant modes of the electromagnetic environment. We observe pronounced current peaks in the transport characteristics of both types of devices and attribute them to the process involving simultaneous tunneling of Cooper pairs and photon emission into the resonant modes. The experimental data are well reproduced with the theoretical models.

DOI: 10.1103/PhysRevB.83.020502 PACS number(s): 74.50.+r, 73.23.−b, 73.63.−b

Charge tunneling in ultrasmall junctions is affected by the electromagnetic environment (EE).[1,2] For example, the same tunnel junction placed in different EE's exhibits different transport characteristics.[3] It was understood that the tunneling charge probes the electromagnetic environment at certain distances, thus forming a coupled junction + environment system.[4] Similar physics governs the single-electron transistor (SET),[1] but now resulting in characteristics that are periodically modulated by the gate voltage.

For single junctions, these ideas were developed into a relatively simple model, nicknamed $P(E)$ theory,[5] in which the function $P(E)$ describes the probability for the tunneling electrons (charges) to exchange energy E with the environment. Due to the progress in nanofabrication, it became possible to engineer an on-chip EE by using various techniques. For example, a high-impedance environment can be created by placing miniature thin-film resistors in the dc leads in the vicinity of the tunnel junction.[6,7] It is also possible to construct an environment with distinct, well-characterized resonance modes.[8,9]

Although the effect of the resonant EE is well understood and received sufficient experimental support[8,9] and theoretical explanations[10] in the case of a single Josephson junction (JJ), clear experimental data for transport properties are still lacking in the case of a superconducting SET (SSET). The SSET coupled to a lossy transmission line was studied experimentally in Ref. 11, and some signatures of the environmental modes were observed. In the present work, we report our transport measurements on single and double Josephson junctions coupled to distinct electromagnetic modes of the environment. Both types of devices reveal a characteristic peak structure in transport that is interpreted to arise from the interaction of the tunneling Cooper pairs with the resonant environment. The experimental data of the SSET is well reproduced by the theory applying the density matrix to Cooper pair tunneling in the presence of (i) the environmental modes, identified in the single JJ experiment, and (ii) the substantial subgap electronic density of states in the superconducting Nb island. The observed resonances appear to be generic for structures having metallic leads on the surface of, for example, Si chips, unless special care is taken to suppress them.

The configuration of our chips is shown in the inset of Fig. 1. The samples consist of $Al/AlO_x/Nb$ tunnel junctions and $Al/AlO_x/Nb/AlO_x/Al$ single-electron transistors made by electron-beam lithography[12] and embedded into Au leads prefabricated photolithographically on a silicon chip. In addition to the Al/Nb junctions, an all-Al junction was also measured. The Si chip of thickness 0.3 mm with a 300-nm-thick oxidized layer on top is placed in a copper sample package forming a ground plane at the bottom of the chip. The Au leads and the ground plane form microstrips on both sides of the junctions or transistors with a wave impedance $Z_0 \approx 40\ \Omega$. The microstrips are bonded with 0.025-mm Au wire to the cryostat wires for dc measurements. The impedance of the bonding wire ($Z_L \sim 200\ \Omega$ at a few tens of GHz) creates an impedance mismatch. Therefore, the microstrips resonate approximately at frequencies $n\omega_0$, where n is an integer and $\omega_0 = \pi c/\sqrt{\varepsilon_e}\ell$ is the fundamental frequency corresponding to the $\lambda/2$ resonance. Here c is the speed of light in vacuum, $\varepsilon_e \approx 7$ is the effective dielectric constant of the microstrip,[13] and $\ell \approx 1.9$ mm is the microstrip length. These numbers give the resonance frequency $\omega_0/2\pi \approx 30$ GHz. With the resistance of each Au lead measured at sub-Kelvin temperature $R_{\mathrm{Au}} \approx 3.5\ \Omega$, we estimate the microstrip resonator quality factor $Q \approx 5$, which is mostly determined by the external impedance of 200 Ω. Measurements were done using a two-probe scheme in a dilution refrigerator at a base temperature of about 40 mK.

A collection of the single-junction dc current-voltage (I-V) characteristics at the subgap voltage is shown in Fig. 1. The common feature of the junctions measured, regardless of the electrode materials, is that at low bias voltage they all exhibit an approximately equidistant peak structure. The peak position does not depend on the junction resistance. The location of the first peak at a bias voltage of $\approx 61\ \mu$V agrees with the estimated resonance frequency ω_0 through the relation $2eV = \hbar\omega_0$ (leading to $\omega_0/2\pi = 29.4$ GHz).

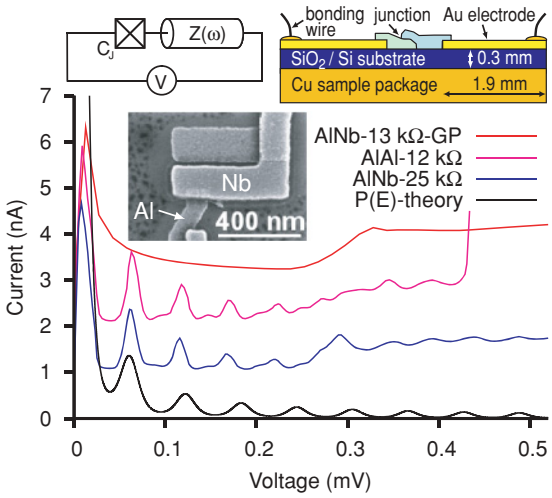

FIG. 1. (Color online) Current as a function of bias voltage through single JJ's embedded in a resonant environment and the $P(E)$ theory result with the quasiparticle tunneling neglected. For one junction, AlNb-13 kΩ-GP, the environmental resonances were suppressed by using a ground plane right beneath the Au leads. The experimental curves are shifted by 1, 2, and 3 nA, respectively, from bottom to top. The normal state resistances in the legend were used to deduce the Josephson coupling energies using the Ambegaokar-Baratoff relation,[14] $C_J = 1$ fF, $\Delta_{\rm Al} = 215\ \mu$eV, $\Delta_{\rm Nb} = 1.15$ meV, and $T = 100$ mK. The Josephson coupling energy of the AlNb-25 kΩ junction is practically the same as of the AlAl-12 kΩ junction ($E_J = 57\ \mu$eV), for which the simulation is made. The EE is characterized in the text. Inset: chip layout (top right, not to scale), equivalent circuit (top left), and scanning electron micrograph of the AlNb single junction.

If a ground plane is placed beneath the leads and separated from them by a thin (300-nm) insulating layer, the environmental resonances become suppressed and the current peaks in the I-V characteristics disappear due to the large shunting capacitance between the Au leads and the ground plane; see the top curve in Fig. 1. We also observe a steplike enhancement of the current roughly above $V = \Delta_{\rm Al}/e$ in both Al/Nb and all-Al JJ's, resulting probably from Andreev tunneling.[15]

We model the single JJ I-V characteristics using the $P(E)$ theory and equivalent circuit shown in the inset of Fig. 1. The electromagnetic environment seen by the JJ is a parallel connection of the junction capacitance C_J and transmission line impedance $Z(\omega) = 2Z_0[Z_L + Z_0\tanh(\gamma\ell)]/[Z_0 + Z_L\tanh(\gamma\ell)]$,[13] where the factor 2 emerges from the fact that we have effectively two equivalent resonators in series, and $\gamma\ell = R_{\rm Au}/2Z_0 + i\pi\omega/\omega_0$. In the simulations, we have used the junction capacitance $C_J = 1$ fF and the fundamental resonance frequency $\omega_0/2\pi = 29.4$ GHz assuming also that the resonances are equidistant. In Fig. 1, we see a reasonably good agreement between the simulated curve and the measured ones for both peak positions and magnitude. The shift of the higher resonant peaks toward the origin visible in the experimental curves can be explained by the fact that for the given lead's geometry, the resonances occur not at multiples of ω_0 but at lower frequencies. This is confirmed by more detailed microstrip analysis performed with MICROWAVE OFFICE. Multiphoton transitions (to the fundamental mode) could also result in a similar peak structure, but are present with negligible magnitudes.

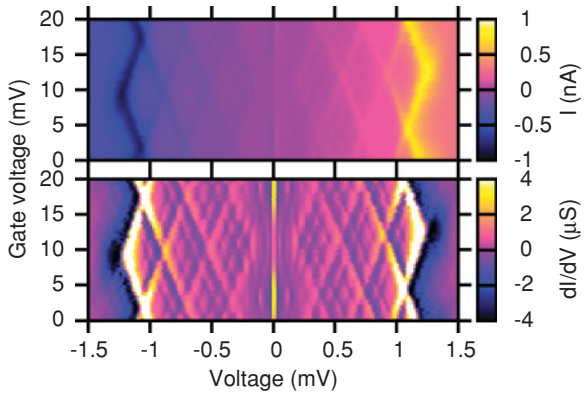

FIG. 2. (Color online) Current (upper panel) and differential conductance dI/dV (lower panel) through the Al-Nb-Al SSET as a function of the gate and bias voltages. The characteristics are e-periodic as a function of the gate and consist of rhombi-shaped cells, which are due to the subgap JQP cycles (see the text), ending with intense normal JQP cycles at higher bias voltages. Differential conductance reveals resonant peak structure in each cell.

We then turn to a characterization of the SSET transport shown in a large scale in Fig. 2. The Josephson-quasiparticle (JQP) current[16] is seen at about $V = \pm 1.2$ mV but also rhombi-shaped cells exist at lower voltages, starting already from 0.18 mV, with a gate modulation period of about 15 mV. The lower voltage structure occurs also due to the JQP processes. Such a multiple JQP peak structure in Al/Nb SSET's has been observed and discussed in earlier works.[17–19] The noteworthy feature here is the structure inside the cells; see also Fig. 3(a).

Our simulations of the SSET's are based on the density-matrix approach (DMA) developed in Ref. 20, with supplements given below. The model describes charge transport via incoherent Cooper-pair tunneling taking place at finite bias voltages. To account for the subgap density of states (DOS) in the niobium island, we use a broadened Bardeen-Cooper-Schrieffer (BCS) DOS of the form[21]

$$n(E) = \left|{\rm Re}\left\{\frac{E - i\Gamma}{\sqrt{(E - i\Gamma)^2 - \Delta_{\rm Nb}^2}}\right\}\right|, \qquad (1)$$

where Γ is a broadening parameter that is adjusted in the simulations to obtain a better fit. At low energies, such a DOS is a constant, $\Gamma/\Delta_{\rm Nb}$, resembling the metallic DOS. Further, we assume that an unpaired electron tunneled into the niobium island relaxes quickly to the Fermi level due to the significant subgap DOS. This kills the asymmetry of the tunneling rates for different parities of the island[22] and results in e-periodic characteristics.

We also see the effects due to nonequilibrium quasiparticles[23] entering the island from the leads at energy $\Delta_{\rm Al}$ or higher. For qualitative modeling, we assume that the electron tunneling rates into and out of the island are equal and described by the expression[24]

$$R(E) = \frac{r}{1 + \exp[-(E + \Delta_{\rm Al} - \Delta_i)/k_BT]}, \qquad (2)$$

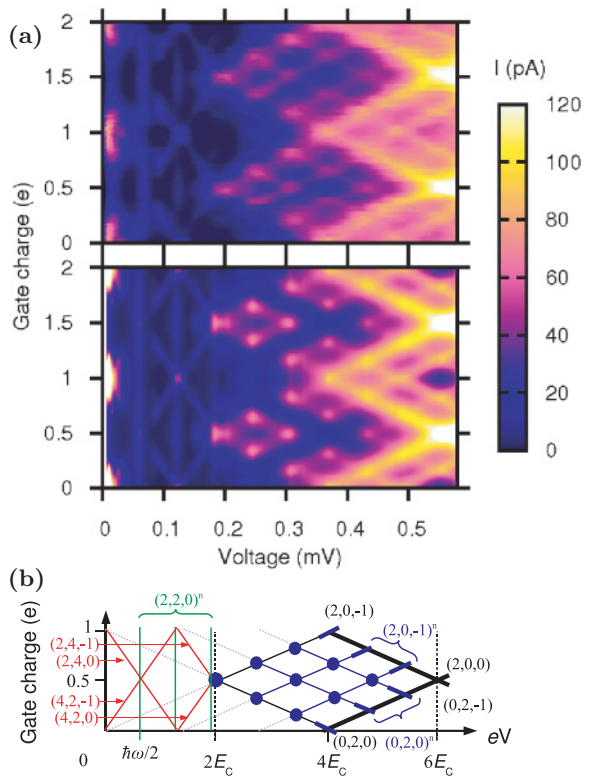

FIG. 3. (Color online) (a) Measured current (upper panel) shown in Fig. 2 but in a smaller scale, and the current calculated by the DMA (lower panel). Since the DMA does not hold in the supercurrent region, the numerical results are shown from 10 μV. The parameters in the simulation are $R_1 = R_2 = 36.5$ kΩ, $E_C = 93$ μeV, $\Delta_{\rm Al} = 215$ μeV, $\Delta_{\rm Nb} = 1.15$ meV, $\Gamma = \Delta_{\rm Nb}/80$, $r = 1/45$ μs, and $T = 100$ mK. The EE seen by the SSET is characterized in the text. (b) Origin of the resonance structure. In a resonant tunneling $(a,b,i)^n$, the charge ae (be) tunnels across the left (right) JJ with the simultaneous excitation of the nth mode, the island charge being initially ie.[20] At low voltages, only the third-order CP tunneling resonances are seen [$(a+b)/2 = 3$], in addition to cotunneling ($a = b$) with the simultaneous excitation of a corresponding mode. At higher voltages, the subgap JQP cycles, enabled by niobium's subgap DOS, first become possible at double resonance points (dots) and eventually nearby thick solid lines.

where Δ_i is the energy gap in the island, E is the energy change in the SSET, and the maximum rate r characterizes the magnitude of the leakage. In the ideal case, practically none of the quasiparticles get through due to large $\Delta_i = \Delta_{\rm Nb}$, however, due to significant subgap DOS, we set $\Delta_i = 0$ and calculate the nonequilibrium part of the quasiparticle tunneling using $R(E)$ as a prefactor of the corresponding Lindblad operators.[20]

Numerical results obtained by the DMA are compared with the experiment in Fig. 3. The Josephson coupling energies are deduced from the transport measurements giving $R_1 + R_2 = 73$ kΩ and assuming that $R_1 = R_2$. The charging energy of the island is obtained from the cell structure giving $E_C \approx 93$ μeV ($C_1 \approx C_2$). To estimate the effective EE seen by the SSET, we use the equivalent circuit shown in the inset of Fig. 1 but with $C_J = C_1/2$. In the DMA, the environmental impedance is included directly in the tunneling rate, similarly to Ref. 8. This approximation neglects the rare multiphoton transitions. To model (non-Markovian) low-frequency background charge fluctuations, we have also averaged the numerical results with respect to the gate charge with a Gaussian distribution of width $4e/100$.

Let us analyze first the charge transport at a higher bias voltage. Due to the broadened DOS in the niobium, the onset of the (subgap) JQP cycle occurs when enough energy can be released to create an excitation on the aluminum side of the JJ's. This leads to the threshold $eV = \Delta_{\rm Al} - E_C$ for the double JQP cycle and $eV = \Delta_{\rm Al} + E_C$ for the ordinary (but subgap) JQP cycle. The resonances appear first at double JQP points (in Fig. 3 at the low voltage corners of the JQP cells, i.e., at $eV = 2E_C \approx 185$ μeV and $Q_0 = e/2 + me$) and approximately above the threshold $eV = \Delta_{\rm Al} + E_C$ as continuous resonance lines. Inside each JQP cell there is a fine structure due to the coupling to the resonant modes of the EE. The origin is that the Cooper-pair tunneling in the JQP process can also be resonant if the extra energy released is absorbed by the environmental mode. This leads to extra JQP-n lines located at $n\hbar\omega_0/e$ above the main resonant voltages, each corresponding to a photon emission to the nth mode. These extra resonances show similar behavior to the main JQP resonances and appear first as dots at double resonance points, and as resonance lines at higher bias voltages. The exact thresholds are $eV = \Delta_{\rm Al} \pm E_C + n\hbar\omega_0/2$ corresponding to double resonances ($-$ sign) and resonance lines ($+$ sign). For the double resonance to occur, two simultaneous resonances corresponding to two different parities of the island charge must coexist, and the resonant states must match. It follows from this that the double JQP-n resonances can occur only inside the triangle-shaped areas starting at $eV = 2E_C$. The subgap JQP structure disappears finally after the onset of the ordinary JQP cycle at $eV \approx \Delta_{\rm Al} + \Delta_{\rm Nb}$ (see Fig. 2). The position of this ordinary JQP is reduced from the ideal one $\Delta_{\rm Al} + \Delta_{\rm Nb} + E_C < eV < \Delta_{\rm Al} + \Delta_{\rm Nb} + 3E_C$ due to the high subgap leakage of Nb-based junctions, which is described by the broadened DOS, and due to the quantum Zeno effect in the charge transport,[20] as near the threshold the quasiparticle rate is high compared to the Josephson coupling energies.

The region of the intermediate voltages (50–200 μV) reveals resonances due to the Cooper-pair cotunneling across both JJ's and a simultaneous photon emission to the first mode, which enhances the current at $V \approx 61$ μV. While the position of the resonance is gate-independent, its magnitude increases when also first- or third-order Cooper-pair tunneling (without photon emission) becomes resonant; see also Fig. 3(b). Also traces of additional modes via such cotunneling can be found at multiples of this voltage. The third-order Cooper-pair tunneling resonances,[20] corresponding to $4e$ tunneling across one and $2e$ tunneling across the other JJ, are seen as sloping resonance lines in the range 80$-$180 μV. These resonances were reported also in earlier works.[25,26]

Finally, we come to the supercurrent region (0–50 μV). The current peaks are e-periodic, resulting from the presence of significant subgap DOS. The number of electrons on the island is described by an integer m. As there is no extra energy related to an odd m, the system tends to minimize the electrostatic energy $(me - Q_0)^2/2C$ through slow higher-order processes. Therefore, it avoids the degeneracy points

$|Q_0 - me| = e$, which enable large supercurrents across the system. As a result, in the absence of external quasiparticle leakage, there should be no significant supercurrent, and it has maxima at $Q_0 = e/2 + me$ (with integer m). This is not the case in the experiment. Indeed, the smallness of the subgap normal-superconductor tunneling current makes it possible that a small leakage current ($1/r$ between a microsecond and a millisecond) opposes the slow higher-order processes and provides strong supercurrent peaks at $Q_0 = e + me$.

In summary, we have observed pronounced current peaks in the SET transport resulting from the Cooper-pair tunneling and simultaneous single-photon emission into the resonant modes. They are seen in a wide range of bias voltages due to the finite electronic subgap DOS in the niobium island. These gate-dependent peaks have the same origin as those observed at a lower bias voltage that do not depend on the gate voltage. Also, all these peaks have their analogs in transport through single Josephson junctions, which were reported earlier. Apparently, the observed resonances may be detrimental to various practical devices as they cause, for example, extra decoherence of quantum bits and errors in charge pumps.

We thank S. Ashhab, D. V. Averin, A. Maassen van den Brink, M. Marthaler, G. Schön, and A. Zagoskin for fruitful discussions. This work was supported by the JSPS through its FIRST Program, JST-CREST and MEXT kakenhi "Quantum Cybernetics." H. Im acknowledges partial support from the National Research Foundation (NRF) of Korea (Grant No. K20901000002-09E0100-00210).

*pashkin@zp.jp.nec.com; on leave from Lebedev Physical Institute, Moscow 119991, Russia.

[1] G.-L. Ingold and Yu. V. Nazarov, in *Single Charge Tunneling: Coulomb Blockade Phenomena in Nanostructures*, edited by H. Grabert and M. H. Devoret (Plenum, New York, 1992), p. 21.

[2] G. Schön and A. D. Zaikin, Phys. Rep. **198**, 237 (1990).

[3] P. Delsing, K. K. Likharev, L. S. Kuzmin, and T. Claeson, Phys. Rev. Lett. **63**, 1180 (1989).

[4] Yu. V. Nazarov, Sov. Phys. JETP **68**, 561 (1989) [Zh. Eksp. Teor. Fiz. **95**, 975 (1989)].

[5] M. H. Devoret, D. Esteve, H. Grabert, G.-L. Ingold, H. Pothier, and C. Urbina, Phys. Rev. Lett. **64**, 1824 (1990).

[6] D. B. Haviland, L. S. Kuzmin, P. Delsing, and T. Claeson, Europhys. Lett. **16**, 103 (1991).

[7] L. S. Kuzmin and D. B. Haviland, Phys. Rev. Lett. **67**, 2890 (1991).

[8] T. Holst, D. Esteve, C. Urbina, and M. H. Devoret, Phys. Rev. Lett. **73**, 3455 (1994).

[9] J. Basset, H. Bouchiat, and R. Deblock, Phys. Rev. Lett. **105**, 166801 (2010).

[10] G.-L. Ingold, H. Grabert, and U. Eberhardt, Phys. Rev. B **50**, 395 (1994).

[11] W. Lu, K. D. Maranowski, and A. J. Rimberg, Phys. Rev. B **65**, 060501 (2002).

[12] H. Im, Yu. A. Pashkin, T. Yamamoto, O. Astafiev, Y. Nakamura, and J. S. Tsai, Appl. Phys. Lett. **88**, 112113 (2006).

[13] D. M. Pozar, *Microwave Engineering*, 3rd ed. (Wiley, Hoboken, NJ, 2005).

[14] V. Ambegaokar and A. Baratoff, Phys. Rev. Lett. **10**, 486 (1963).

[15] F. W. J. Hekking and Yu. V. Nazarov, Phys. Rev. B **49**, 6847 (1994).

[16] T. A. Fulton, P. L. Gammel, D. J. Bishop, L. N. Dunkleberger, and G. J. Dolan, Phys. Rev. Lett. **63**, 1307 (1989).

[17] Y. Harada, D. B. Haviland, P. Delsing, C. D. Chen, and T. Claeson, Appl. Phys. Lett. **65**, 636 (1994).

[18] R. Dolata, H. Scherer, A. B. Zorin, and J. Niemeyer, Appl. Phys. Lett. **80**, 2776 (2002).

[19] J. J. Toppari, T. Kühn, A. P. Halvari, J. Kinnunen, M. Leskinen, and G. S. Paraoanu, Phys. Rev. B **76**, 172505 (2007).

[20] J. Leppäkangas and E. Thuneberg, Phys. Rev. B **78**, 144518 (2008).

[21] R. C. Dynes, J. P. Garno, G. B. Hertel, and T. P. Orlando, Phys. Rev. Lett. **53**, 2437 (1984).

[22] J. Siewert and G. Schön, Phys. Rev. B **54**, 7421 (1996).

[23] J. M. Martinis, M. Ansmann, and J. Aumentado, Phys. Rev. Lett. **103**, 097002 (2009).

[24] G. Schön and A. D. Zaikin, Europhys. Lett. **26**, 695 (1994).

[25] P. Joyez, Ph.D. thesis, Paris 6 University (1995).

[26] P.-M. Billangeon, F. Pierre, H. Bouchiat, and R. Deblock, Phys. Rev. Lett. **98**, 216802 (2007).